Eur. Phys. J. D (2023) 77:132
https://doi.org/10.1140/epjd/s10053-023-00715-4

THE EUROPEAN PHYSICAL JOURNAL D

Regular Article – Optical Phenomena and Photonics

Quadrifocal diffractive lenses based on the aperiodic silver mean sequence

Adrián Garmendía-Martínez[1,a], Walter D. Furlan[2], Juan C. Castro-Palacio[1], Juan A. Monsoriu[1], and Vicente Ferrando[1]

[1] Centro de Tecnologías Físicas, Universitat Politècnica de València, 46022 Valencia, Spain
[2] Departamento de Óptica y Optometría y Ciencias de la Visión, Universitat de València, 46100 Valencia, Spain

Received 2 May 2023 / Accepted 23 June 2023 / Published online 10 July 2023
© The Author(s) 2023

Abstract. In this work, we present a new quadrifocal diffractive lens designed using the silver mean sequence. The focusing properties of these aperiodic diffractive lenses coined silver mean zone plates are analytically examined. It is demonstrated that, under monochromatic illumination, these lenses present four foci located at certain reduced axial positions given by the Pell numbers that can be correlated with the silver mean sequence. This distinctive optical characteristic is experimentally confirmed.

1 Introduction

A renewed interest in diffractive optical elements (DOEs) has been experienced by the scientific community in the last years because these elements are essential as image forming setups that are used in THz applications [1,2], soft X-ray microscopy [3,4], astronomy [5,6], lithography [7] and ophthalmology [8,9], among others. A Zone Plate (ZP) [10], the simplest form of a diffractive lens, is characterized by a series of concentric transparent and opaque annular rings distributed periodically along the square of the radial coordinate, so the area of each annular zone is a constant. Under plane wave illumination, this distribution of zones produced by diffraction a set of foci located along the optical axis. To improve diffraction efficiency, binary phase ZPs [11] and kinoform lenses [12] (ZPs with a sawtooth profile) can be used. With the latter configuration, it can be achieved theoretically that all the energy concentrates on a single focus for the design wavelength. Photon Sieves [13] have been also implemented to improve diffraction efficiency. In this application, the transparent annular zones of amplitude ZPs are replaced by a disjoint set of holes.

Within this context, fractal zone plates (FZPs) were proposed by our group as a new promising structured diffractive lenses [14]. Under certain circumstances, a FZP can be considered as a conventional Fresnel zone plate with certain missing zones. The resulting structure is characterized by its fractal profile along the square of the radial coordinate. The axial irradiance provided by a FZP when illuminated with a parallel wavefront presents multiple foci creating a focal volume with an internal fractal structure, reproducing the self-similarity of the originating FZP. Imaging properties of FZP were also investigated. Interestingly, under polychromatic illumination a FZP produces a substantial increase in the depth of field and a noticeable reduction in the chromatic aberration compared with a Fresnel zone plate of the same focal distance [15]. Additionally, in order to design optimized optical systems, different mechanisms to control the diffraction efficiency of fractal lenses have been proposed in different publications. We have shown that the diffraction efficiency of a FZP can be controlled by amplitude modulation, resulting in new elements called fractal photon sieves [16] and also by fractal kinoform zone plates known as Devi'ls lenses [17]. These designs were the basis of new fractal intraocular lenses [18,19] and fractal contact lenses [20,21].

In addition to fractal elements, there are numerous aperiodic sequences [22,23] with which diffractive lenses can be structured. Diffractive lenses based on the Fibonacci [24] and m-Bonacci [25] sequences display focal splitting with respect to periodically structured ones. Other aperiodic sequences with which we have designed multifocal diffractive lenses are the Thue–Morse [26], the Rudin–Shapiro [27] and the Walsh functions [28]. Another interesting mathematical generator is the generalized precious mean sequence which includes the silver mean sequence [29,30]. This sequence has been employed in the development of different aperiodic systems, such as photonic and phononic quasicrystals [31,32].

In this paper, we show that silver mean zone plates (SMZPs), i.e., ZPs with a distribution of zones based on the silver mean sequence, are intrinsically quadrifocals. The corresponding foci are located at reduced

[a] e-mail: agarm13a@upvnet.upv.es (corresponding author)

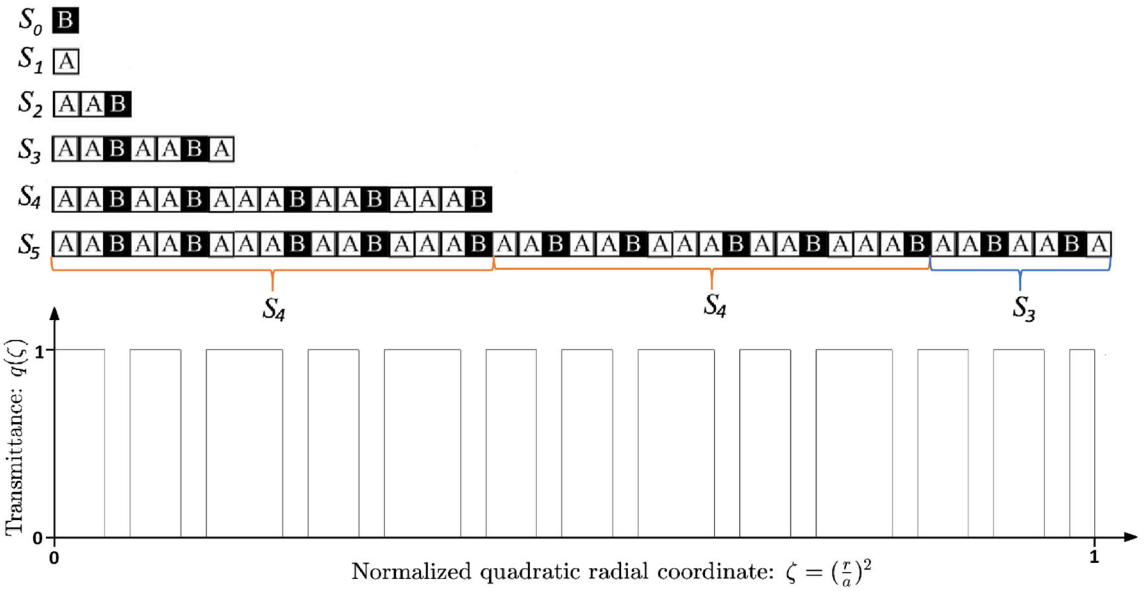

Fig. 1 Generation of the silver mean sequence up to order $n = 5$ and the transmittance function $q(\zeta)$ of the corresponding SMZP

axial positions given by de Pell numbers that can be correlated with the involved aperiodic sequence. This property is experimentally verified and compared with the theoretical prediction computed numerically. Both results are in excellent agreement.

2 Silver mean zone plates design

The Pell numbers, $P_n = \{0, 1, 2, 5, 12, 29, 70, ...\}$ are obtained from the recurrence relation $P_n = 2P_{n-1} + P_{n-2}$ $(n \geq 2)$, starting from the seeds $P_0 = 0$ and $P_1 = 1$ [33,34]. The silver ratio is defined as the limit of the ratio between two consecutive Pell numbers:

$$\phi = \lim_{n\to\infty} \frac{P_n}{P_{n-1}} = 1 + \sqrt{2} \tag{1}$$

Based on Pell numbers, the so-called silver mean sequence can be generated from two seeds $S_0 = B$ and $S_1 = A$ as shown in Fig. 1. Each element of the series is obtained from the following concatenation rule: $S_n = \{S_{n-1}S_{n-1}S_{n-2}\}$ for $n \geq 2$. This aperiodic sequence can also be generated iteratively by applying the substitution rules $g(A) = AAB$ and $g(B) = A$, that is, $S_2 = AAB$, $S_3 = AABAABA$, $S_4 = AABAABAAABAABAAAB$, etc. Note that the total number of elements of a given sequence of order n is $P_n + P_{n-1}$, which results from the sum of P_n elements "A" plus P_{n-1} elements "B."

When designing SMZPs, each of these sequences can be used to define the transmission generating function $q(\zeta)$, with compact support on the interval $\zeta \in [0, 1]$. This interval is partitioned in $P_n + P_{n-1}$ sub-intervals of length $d_n = \frac{1}{P_n+P_{n-1}}$. The transmittance value, $t_{n,j}$, that takes at the j-th sub-interval is associated with the element $S_{n,j}$, being $t_{n,j} = 1$, when $S_{n,j}$, is "A" and $t_{n,j} = 0$, when $S_{n,j}$, is "B" (see Fig. 1). In mathematical terms, the transmittance function, $q(\zeta)$, can be written as:

$$q(\zeta) = \sum_{j=1}^{P_n+P_{n-1}} t_{n,j} rect\left[\frac{\zeta - (j - 1/2)d_n}{d_n}\right] \tag{2}$$

where $\zeta = (\frac{r}{a})^2$ is the normalized quadratic radial coordinate, r is the radial coordinate, a is the radius of the lens and *rect* is the rectangular function. Figure 2 shows a ZP based on the silver mean sequence of order $n = 5$.

Note that the number of zones of a SMZP of order n coincides with $P_n + P_{n-1}$, being P_n and P_{n-1} the number of transparent and opaque zones, respectively. We have found that not only the number of zones is related to the Pell numbers but also the foci distribution produced by the diffractive lens along the optical axis. For this, the focusing properties of a SMZP were studied numerically, using the Fresnel–Kirchhoff formula [35, 36]:

$$U(x, y, z) = -\frac{e^{-ikz}e^{-\frac{ik}{2z}(x^2+y^2)}}{i\lambda z} \iint_{-\infty}^{\infty} q(x_0, y_0)e^{\frac{-ik}{2z}(x_0^2+y_0^2)}e^{\frac{ik}{z}(xx_0+yy_0)}dx_0dy_0 \tag{3}$$

where $U(x, y, z)$ is the amplitude of the diffracted field at position (x, y, z), $k = \frac{2\pi}{\lambda}$ is the angular wave number, λ is the wavelength and the integration limits correspond to the opening dimensions. From Eq. (3), the irradiance can be obtained as the square of the amplitude for the diffracted field. Using normalized coordi-

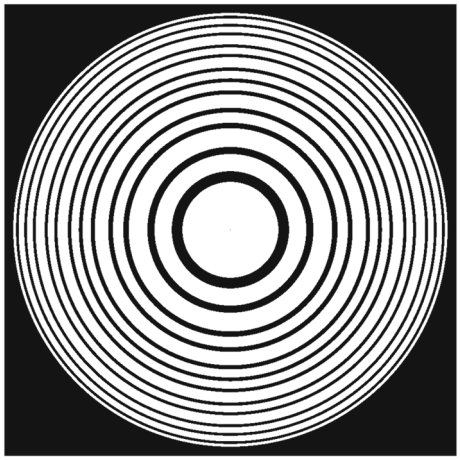

Fig. 2 Silver mean zone plate of order $n = 5$

nates for the pupil plane as $\bar{x}_0 = \frac{x_0}{a}$, $\bar{y}_0 = \frac{y_0}{a}$, the irradiance is given by

$$I(x, y, u) = 4u^2 \left| \iint_{-\infty}^{\infty} q(\bar{x}_0, \bar{y}_0) e^{i2\pi u(\bar{x}_0^2 + \bar{y}_0^2)} e^{-i2\pi 2u(x\bar{x}_0 + y\bar{y}_0)} \mathrm{d}\bar{x}_0 \mathrm{d}\bar{y}_0 \right|^2 \tag{4}$$

where $u = \frac{a^2}{2\lambda z}$ is the reduced axial coordinate. If only the irradiance along the propagation axis is considered and the diffractive element has radial symmetry, Eq. (4) becomes

$$I(u) = 4\pi^2 u^2 \left| \int_0^1 q(\zeta) e^{-i2\pi u\zeta} d\zeta \right|^2 \tag{5}$$

Figure 3 shows the axial normalized irradiance distributions, corresponding to the first-order diffraction foci, computed for SMZPs of orders $n = 4, 5, 6$. The axial irradiance was obtained from Eq. (5) using the 1D Fast Fourier Transform method, since this method requires low computation time compared to other numerical methods commonly used [36]. As can be seen, SMZPs

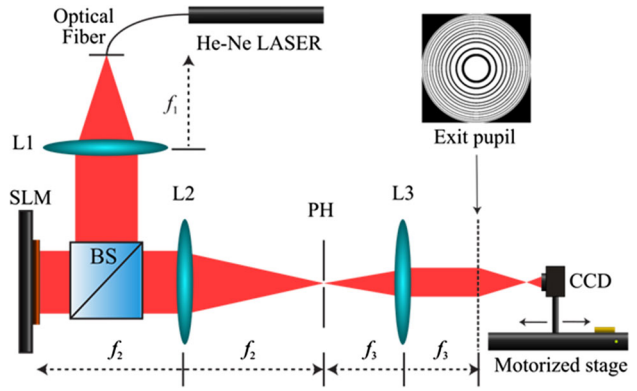

Fig. 4 Scheme of the experimental setup used to study the focusing properties of SMZPs

produce the formation of four foci distributed along the axis. Note that the corresponding reduced focal lengths u_a, u_b, u_c, and u_d approximate to P_{n-1}, $P_{n-1} + P_{n-2}$, $2P_{n-1}$ and P_n, respectively. Therefore, the ratio between the focal distances is $\frac{u_d}{u_a} \approx \phi = 1 + \sqrt{2}$, $\frac{u_c}{u_a} \approx 2$, and $\frac{u_b}{u_a} \approx 1 + \frac{1}{\phi} = \sqrt{2}$, respectively. The higher the order of the sequence, the better these approximations will be. For example, for $n = 6$, the discrepancy between these approximations and the corresponding ratio between the focal distances is less than 0.07%.

3 Experimental setup and results

The focusing properties of SMZPs have been studied experimentally using the setup schemed in Fig. 4. The studied lens was implemented in the liquid crystal spatial light modulator (SLM) (Holoeye PLUTO, 1920 × 1080 pixels, pixel size 8 μm, 8-bit gray-level) operating in phase-only modulation mode. A collimated and linearly polarized beam from an He-Ne Laser ($\lambda = 633$ nm) illuminates the SLM. The SLM is programmed to show a linear phase grating in the zones with transmittance 1, while the rest of the display shows a constant phase. In this way, white zones are deflected to

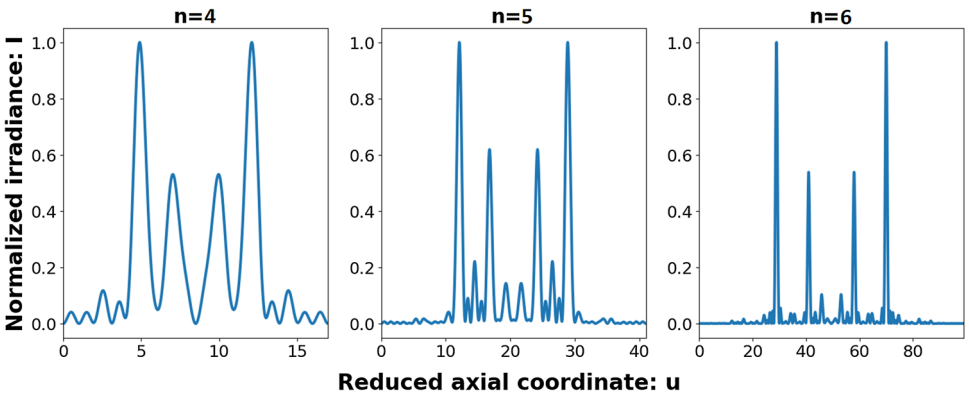

Fig. 3 Normalized irradiance *versus* reduced axial coordinate of silver mean zone plates of orders $n = 4, 5, 6$

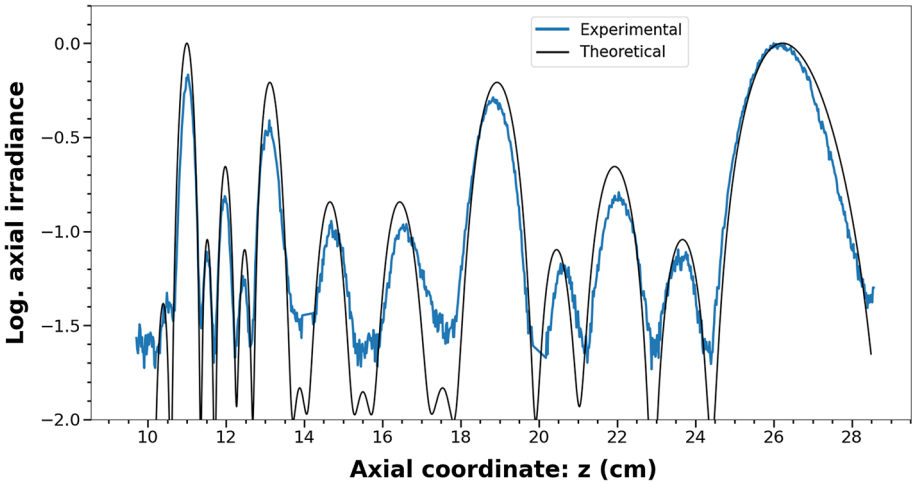

Fig. 5 Comparison of numerical and experimental axial irradiance of a SMZP of order 5

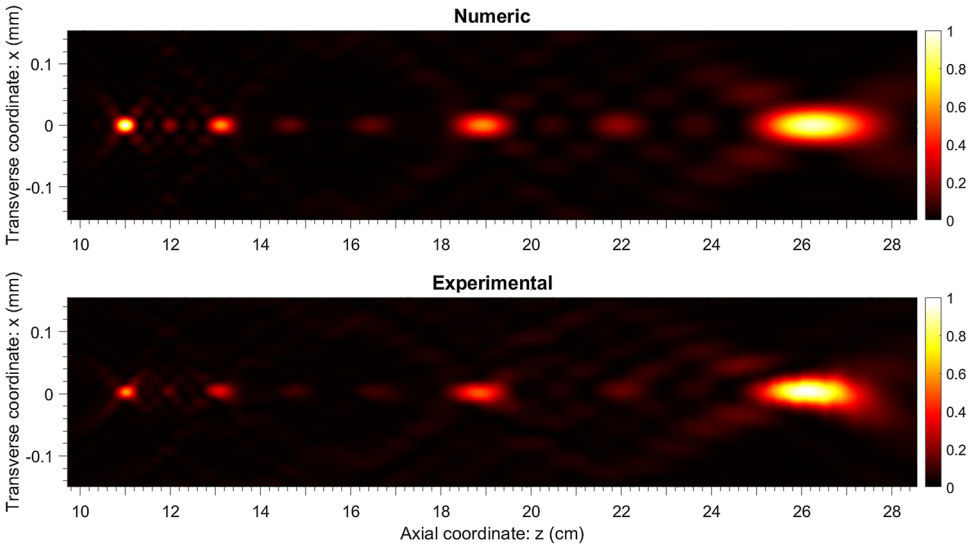

Fig. 6 Evolution of the transverse intensity distribution produced by a SMZP of order 5

the first diffractive order of the grating, while black zones are reflected specularly (zero diffractive order). The SLM plane is imaged through a telescopic system (L2 and L3). The SLM is slightly tilted to correct the linear phase, and a pinhole (PH) is positioned at the Fourier plane to eliminate all diffraction orders of the linear phase grating except order +1. The PH also prevents noise from the specular reflection (zero diffractive order) and the pixelated structure of the SLM (higher diffraction orders). In this way, the studied lens transmittance is projected at the pupil plane and its focusing profile can be captured along the axis by a camera sensor mounted on a motorized stage.

We have experimentally characterized a SMZP of order $n = 5$ and a radius $a = 2.01$ mm. The experimental axial irradiance provided by this ZP is shown in Fig. 5 along with the irradiance obtained numerically for comparison purposes. It can be seen that the SMZP provides four foci whose axial positions are $z_a = 26.47$ cm, $z_b = 18.91$ cm, $z_c = 13.12$ cm and $z_d = 10.91$ cm. The corresponding experimental reduced axial coordinates, $u = \frac{a^2}{2\lambda z}$, are $u_a = 12.00$, $u_b = 16.80$, $u_c = 24.21$ and $u_d = 29.11$, respectively. As predicted from the theoretical analysis, the location of each of these foci approximates to $u_a \approx 12 = P_4$, $u_b \approx 17 = P_4 + P_3$, $u_c \approx 24 = 2P_4$, and $u_d \approx 29 = P_5$. The ratio between the positions of the fourth and first foci approximates to the silver ratio $\phi \approx \frac{u_d}{u_a} = 2.426$, while $\frac{u_b}{u_a} = 1.44 \approx \sqrt{2}$ and $\frac{u_b}{u_a} = 2.02 \approx 2$.

To provide a more extensive study of the focusing characteristics of the SMZP, the transversal irradiance distribution in the xz plane was also computed numerically from Eq. (4) using the 2D Fast Fourier Transform method and captured experimentally (Fig. 6). As it can be seen, both results are in full agreement confirming the quadrifocal behavior of the lens as well as the consistent ratios between its focal positions.

4 Conclusions

A zone plate based on the silver mean sequence has been presented in this study. It is shown both theoretically and experimentally that a SMZP produces four foci along the optical axis. It has been demonstrated that these focal lengths are related to the Pell numbers and that the ratio between the fourth and first focus positions approximates the silver ratio. We believe that a diffractive lens based on this aperiodic sequence can have a wide range of applications, such as X-ray microscopy, THz imaging and ophthalmology. In fact, our next step is to design a kinoform-type diffractive structure based on this sequence to achieve an extended depth of focus (EDOF) intraocular lens.

Author contributions

All authors contributed equally to this work.

Funding Information Open Access funding provided thanks to the CRUE-CSIC agreement with Springer Nature.

Data Availability Statement This manuscript has no associated data, or the data will not be deposited. [Authors' comment: With respect the data availability, the procedure to obtain the numerical results is detailed in the article, so there is no need to provide data associated to them. On the other hand, the experimental captures don't provide any relevant information aside from the one already shown in Figures 5 and 6.]

Declarations

Conflict of interest This work was supported by the Ministerio de Ciencia e Innovación de España (grant 192 PID2019-107391RB-I00) and by Generalitat Valenciana (grant CIPROM/2022/30), Spain. A.G.M. acknowledges the financial support from the Generalitat Valenciana (GRISOLIAP/2021/121).

Open Access This article is licensed under a Creative Commons Attribution 4.0 International License, which permits use, sharing, adaptation, distribution and reproduction in any medium or format, as long as you give appropriate credit to the original author(s) and the source, provide a link to the Creative Commons licence, and indicate if changes were made. The images or other third party material in this article are included in the article's Creative Commons licence, unless indicated otherwise in a credit line to the material. If material is not included in the article's Creative Commons licence and your intended use is not permitted by statutory regulation or exceeds the permitted use, you will need to obtain permission directly from the copyright holder. To view a copy of this licence, visit http://creativecommons.org/licenses/by/4.0/.

References

1. S. Wang, X.-C. Zhang, Terahertz technology: terahertz tomographic imaging with a Fresnel lens. Opt. Photon. News **13**(12), 59 (2002)
2. W.D. Furlan, V. Ferrando, J.A. Monsoriu, P. Zagrajek, E.Z. Czerwińska, M. Szustakowski, 3d printed diffractive terahertz lenses. Opt. Lett. **41**(8), 1748–1751 (2016)
3. Y. Wang, W. Yun, C. Jacobsen, Achromatic Fresnel optics for wideband extreme-ultraviolet and X-ray imaging. Nature **424**, 50–53 (2003)
4. L. Kipp et al., Sharper images by focusing soft X-rays with photon sieves. Nature **414**, 184–188 (2001)
5. R.A. Hyde, Eyeglass. 1. very large aperture diffractive telescopes. Appl. Opt. **38**(19), 4198–4212 (1999)
6. G. Andersen, Large optical photon sieve. Opt. Lett. **30**(22), 2976–2978 (2005)
7. R. Menon, D. Gil, G. Barbastathis, H.I. Smith, Photon-sieve lithography. J. Opt. Soc. Am. A **22**(2), 342–345 (2005)
8. J.L. Alio, A.B. Plaza-Puche, R. Férnandez-Buenaga, J. Pikkel, M. Maldonado, Multifocal intraocular lenses: an overview. Survey Ophthalmol. **62**(5), 611–634 (2017)
9. W.D. Furlan, D. Montagud, V. Ferrando, S. García-Delpech, J.A. Monsoriu, Multifocal intraocular lenses: an overview. Sci. Rep. **11**(1) (2021)
10. J. Ojeda Castañeda, C. Gomez-Reino (eds.), *Selected Papers on Zone Plates* (SPIE Optical Engineering Press, Washington, 1996)
11. Y. Geints, E. Panina, I. Minin, O. Minin, Study of focusing parameters of wavelength-scale binary phase Fresnel zone plate. J. Opt. **23**, 065101 (2021)
12. W. Sun et al., X-ray propagation through a kinoform lens. J. Synchrotron Rad. **29**, 1338–1343 (2022)
13. C. Wang, T. Sun, D. Pu, F. Xu, C. Wang, Full-visible achromatic imaging with a single dual-pinhole-coded diffractive photon sieve. Opt. Express **29**(18), 28549–28561 (2021)
14. G. Saavedra, W. Furlan, J. Monsoriu, Fractal zone plates. Opt. Lett. **28**, 971–3 (2003)
15. W.D. Furlan, G. Saavedra, J.A. Monsoriu, White-light imaging with fractal zone plates. Opt. Lett. **32**(15), 2109–2111 (2007)
16. F. Giménez, J.A. Monsoriu, W.D. Furlan, A. Pons, Fractal photon sieve. Opt. Express **14**(25), 11958–11963 (2006)
17. J.A. Monsoriu, W.D. Furlan, G. Saavedra, F. Giménez, Devil's lenses. Opt. Express **15**(21), 13858–13864 (2007)
18. L. Remon, S. Garcia-Delpech, P. Udaondo, V. Ferrando, J. Monsoriu, W. Furlan, Fractal-structured multifocal intraocular lens. PLOS One **13**, 0200197 (2018)
19. W.D. Furlan, A. Martínez-Espert, D. Montagud-Martínez, V. Ferrando, S. García-Delpech, J.A. Monsoriu, Optical performance of a new design of a trifocal intraocular lens based on the devil's diffractive lens. Biomed. Opt. Express **14**(5), 2365–2374 (2023)
20. M. Rodriguez-Vallejo, J. Benlloch, A. Pons, J. Monsoriu, W. Furlan, The effect of fractal contact lenses on peripheral refraction in myopic model eyes. Curr. Eye Res. **39**, 1151–1160 (2014)
21. M. Rodriguez-Vallejo, D. Montagud, J. Monsoriu, V. Ferrando, W. Furlan, Relative peripheral myopia

induced by fractal contact lenses. Curr. Eye Res. **43**, 1–8 (2018)
22. E. Macia, The role of aperiodic order in science and technology. Rep. Prog. Phys. **69**, 397–441 (2006)
23. E. Macia, Exploiting aperiodic designs in nanophotonic devices. Rep. Prog. Phys. Phys. Soc. **75**, 1036502 (2012)
24. J.A. Monsoriu, A. Calatayud, L. Remon, W. Furlan, G. Saavedra, P. Andrés, Bifocal Fibonacci diffractive lenses. Photonics J IEEE **5**, 3400106 (2013)
25. F. Machado, V. Ferrando, W.D. Furlan, J.A. Monsoriu, Diffractive m-bonacci lenses. Opt. Express **25**(7), 8267–8273 (2017)
26. V. Ferrando, F. Gimenez, W. Furlan, J. Monsoriu, Bifractal focusing and imaging properties of Thue-Morse zone plates. Opt. Express **23**, 19846–19853 (2015)
27. T. Xia, M. Ni, S. Cheng, J. Yan, S. Tao, Polychromatic focusing properties of Rudin-Shapiro zone plates (2017), pp. 1–4
28. F. Machado, V. Ferrando, F. Gimenez, W. Furlan, J. Monsoriu, Multiple-plane image formation by Walsh zone plates. Opt. Express **26**, 21210 (2018)
29. T. Xia, S. Cheng, S. Tao, The generalized mean zone plate. Laser Phys. **28**, 066201 (2018)
30. T. Xia, S. Tao, S. Chen, Twin equal-intensity foci with the same resolution generated by a modified precious mean zone plate. J. Opt. Soc. Am. A **37**, 1067–1074 (2020)
31. I. Gahramanov, E. Asgerov, A remark on the trace-map for the silver mean sequence. Mod. Phys. Lett. B **27**, 1350107 (2010)
32. A.K.M. Farhat, L. Morini, M. Gei, Silver-mean canonical quasicrystalline-generated phononic waveguides. J. Sound Vib. **523**, 116679 (2022)
33. A.F. Horadam, Pell identities. Fibonacci Q **9**(3), 245–252 (1971)
34. T. Koshy, *Pell and Pell-Lucas Numbers with Applications* (Springer, New York, 2014)
35. J.W. Goodman, *Introducción a la óptica de Fourier* (Uned Editorial, Madrid, 2008)
36. A. Garmendía-Martínez, F.M. Muñoz-Pérez, W.D. Furlan, F. Giménez, J.C. Castro-Palacio, J.A. Monsoriu, V. Ferrando, Comparative study of numerical methods for solving the Fresnel integral in aperiodic diffractive lenses. Mathematics **11**(4), 946 (2023)